Available online at www.sciencedirect.com
ScienceDirect
Journal of Pharmaceutical and Biomedical Analysis 47 (2008) 312–319
JOURNAL OF PHARMACEUTICAL AND BIOMEDICAL ANALYSIS
www.elsevier.com/locate/jpba

A high-temperature liquid chromatographic reactor approach for investigating the solvolytic stability of a pharmaceutical compound and an investigation of its retention behavior on a C18-modified zirconia stationary phase

Peter J. Skrdla *, Angela Bopra [1], Tyson Chasse, Tao Wang

Merck & Co., Inc., P.O. Box 2000, RY818-C215 Rahway, NJ 07065, United States

Received 28 November 2007; received in revised form 10 January 2008; accepted 13 January 2008
Available online 19 January 2008

Abstract

The solvolysis kinetics of a developmental active pharmaceutical ingredient (API) were investigated using a high temperature (HT)-HPLC reactor approach to determine whether it might be possible to use the technique to efficiently screen the relative stabilities of typical APIs (particularly those that are stable at the column temperatures achievable on most HPLC systems and over durations of less than 60 min—a reasonable upper limit for typical method run time). It was discovered that the on-column API degradation kinetics better obeyed a second-order model than a first-order one. Employing a newly developed mathematical treatment, the apparent activation energy for the process was determined to be 85.7 ± 1.6 kJ/mol; the apparent frequency factor was found to be $(3.9 \pm 0.4) \times 10^4\ s^{-1}$. The retention mechanism of the API on the C18-modified zirconia column (ZirChrom® Diamondbond™-C18) was investigated using a van't Hoff analysis. It was discovered that the logarithm of the retention factor (following correction for the gradient elution of the assay method) exhibited a quadratic dependence on the reciprocal of the absolute temperature. While the retention was found to be predominantly enthalpically driven over the majority of temperatures investigated in this study (ranging from 40 to 200 °C), a regression fit of the curve predicted a maximum at ~20 °C, indicative of a transition from predominantly enthalpically controlled retention to a mainly entropically driven mechanism. A table summarizing the thermodynamic retention parameters at each experimental column temperature is provided. Finally, the preliminary application of the HT-HPLC reactor approach to the study of degradation kinetics of other APIs is discussed in terms of some unexpected findings obtained using the zirconia column.

Keywords: On-column reaction; Degradation kinetics; High-temperature HPLC; Chromatographic reactor; High-temperature oven; Zirconia column; PRP-1 stationary phase

1. Introduction

In a previous work, it was discussed how the implementation of a "chromatographic reactor" approach might be advantageous over performing a traditional Arrhenius-type analysis using solution-phase "batch reactor" data, for quickly obtaining the complete kinetic characterization of a given (hydrolysis/solvolysis) degradation pathway for an active pharmaceutical ingredient (API) [1]. That is because a chromatographic reactor utilizes an analytical-scale column as both a flow-through reactor and, simultaneously, as a separation medium for the reactant(s) and product(s) [1–3]. In chromatographic reactor kinetic experiments, the reaction time (i.e., the API retention time) and reaction temperature are inherently varied at the same time (because retention time is affected by the column temperature). For this reason, the approach seemingly lends itself to efficiently screening compounds based on their relative stability (or lability). However, a key limitation of the approach, for HPLC applications (as opposed to GC reactors), has traditionally been the upper operating temperature of most chromatographic columns and the highest column compartment temperature achievable by most HPLC systems, as set by the manufacturer

* Corresponding author. Tel.: +1 732 594 2491; fax: +1 732 594 3887.
E-mail address: peter_skrdla@merck.com (P.J. Skrdla).
[1] Present address: Department of Chemistry, Grand Valley State University, Allendale, MI 49401, United States.

0731-7085/$ – see front matter © 2008 Elsevier B.V. All rights reserved.
doi:10.1016/j.jpba.2008.01.022

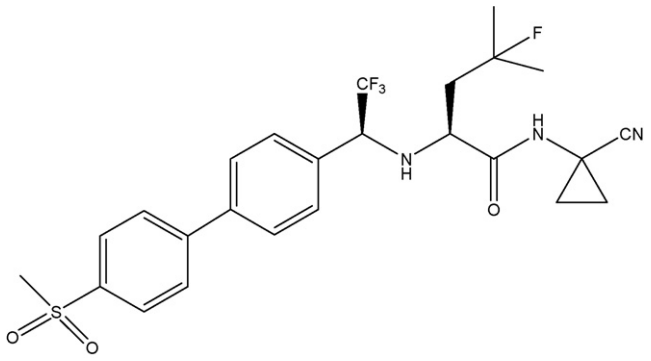

Fig. 1. Molecular structure of Compound A.

(both are typically max. ~80 °C). In this work, a high temperature (HT)-HPLC chromatographic reactor approach is used to investigate the on-column degradation kinetics of an API that is more chemically stable than the one used in the earlier study, performed using more standard HPLC equipment [1]. With the use of an external column oven and a zirconia-based stationary phase, temperatures reaching 200 °C can be routinely accessed [4–6].

The combination of a Selerity Technologies® HT column oven and a ZirChrom® Diamondbond™-C18 column were utilized in the present work to study the kinetics of the thermal degradation (solvolysis) of the API shown in Fig. 1, referred to as "Compound A" for the purposes of this work. Additionally, the retention mechanism of Compound A on the zirconia-based stationary phase was investigated using a van't Hoff analysis. In the following section, the mathematical equations used to treat the kinetic and thermodynamic data from these studies, covering temperatures in the range 40–200 °C (in each case), are outlined. Later in the paper, preliminary HT kinetic data obtained for some other APIs on the same, zirconia-based column are presented and the data is discussed in light of some unusual findings. Finally, the unusual results obtained on the zirconia column for two of the additional compounds are compared to those obtained using a different, non-zirconia-based stationary phase.

2. Theory

2.1. Kinetic treatment of "Reaction Chromatogram" data obtained for the on-column degradation of Compound A

In previous works [7–10], a model for treating first-order/pseudo-first-order chromatographic reactor kinetic data was derived. It can be written as follows:

$$\frac{1}{T} = -\frac{R}{E'_a}\ln\left(\frac{1}{t_R}\ln\left(\frac{A_0}{A}\right)\right) + \frac{R}{E'_a}\ln(\Lambda') \quad (1)$$

where R is the universal gas constant, E'_a is the *apparent* activation energy, Λ' is the *apparent* frequency factor (Arrhenius constant), A is the API peak area (which is directly proportional to concentration) at absolute temperature T and retention time t_R, and A_0 is the peak area of the API at a column temperature where no degradation occurs (taken to be 40 °C in this work, the lowest temperature investigated; by carefully examining the chromatographic baseline and the API peak shape at this temperature, it is clear that the amount of on-column degradation is negligible—less than two tenths of a percent).

In order to treat second-order reaction data, one can follow a similar derivation procedure employing the following integrated rate expression for an *apparent* second-order rate constant, k':

$$k' = \frac{1}{t_R}\left(\frac{1}{A} - \frac{1}{A_0}\right) \quad (2)$$

Note that since use of either the retention time (t_R), the column void time (t_0) or the corrected retention time ($t_R - t_0$) did not significantly affect the quality of the kinetic curve fits discussed later in this work, it is likely that the reaction kinetics of Compound A obey the same mechanism in both the stationary and mobile phases. For that reason, t_R is taken to be the (combined/overall) reaction time for the purposes of this work.

The Arrhenius equation may be written as shown below so that E'_a is an expression of T, Λ' and k':

$$E'_a = -RT\ln\left(\frac{k'}{\Lambda'}\right) \quad (3)$$

Substituting Eq. (2) into Eq. (3), one obtains the following result:

$$E'_a = -RT\ln\left(\frac{1}{\Lambda' t_R}\left(\frac{1}{A} - \frac{1}{A_0}\right)\right) \quad (4)$$

Dividing both sides of Eq. (4) by the term, $E'_a T$, yields the desired result for fitting second-order chromatographic reactor kinetic data:

$$\frac{1}{T} = -\frac{R}{E'_a}\ln\left(\frac{1}{t_R}\left(\frac{1}{A} - \frac{1}{A_0}\right)\right) + \frac{R}{E'_a}\ln(\Lambda') \quad (5)$$

From Eq. (5), one can see that by simply constructing a plot of $1/T$ versus $\ln\left(\frac{1}{t_R}\left(\frac{1}{A} - \frac{1}{A_0}\right)\right)$, it is possible to determine the values of E'_a and Λ' from the slope and vertical axis intercept, respectively, of a linear regression fit of the kinetic data, i.e., (A, t_R, T) triplets. An equivalent form of Eq. (5), not used in this work, is:

$$\ln\left(\frac{1}{t_R}\left(\frac{1}{A} - \frac{1}{A_0}\right)\right) = -\frac{E'_a}{RT} + \ln(\Lambda') \quad (6)$$

whereby the reciprocal temperature can be plotted on the abscissa.

2.2. Mathematical treatment for the thermodynamics of retention of Compound A

The relationship between the retention factor, $k_p = \left(\frac{t_R - t_0}{t_0}\right)$, of a solute and the absolute column temperature, T, can be described using the van't Hoff equation (e.g., [11] and references therein):

$$\ln(k_p) = -\frac{\Delta H}{RT} + \frac{\Delta S}{R} + \ln(\Phi) \quad (7)$$

where Φ is the phase ratio and ΔH and ΔS are the change in enthalpy and entropy, respectively, associated with a given solute as it partitions from the mobile phase into the stationary phase.

Typically, a plot of $\ln(k_p)$ versus $1/T$ will be linear if a single, dominant retention mechanism drives the separation. In the case of a linear van't Hoff relationship, the system can be described by a single value of ΔH and of ΔS over the entire temperature range studied; these parameters are extracted from the slope and vertical axis intercept (respectively) of the plot.

In dealing with non-linear van't Hoff plots, Horváth and co-workers [12] have described a mathematical treatment that allows the extraction of the thermodynamic parameters, ΔH, ΔS and ΔC_p (the last term represents the change in heat capacity), from a *quadratic* regression fit of the $\ln(k_p)$ versus $1/T$ data, using the equation below:

$$\ln(k_p) = a + \frac{b}{T} + \frac{c}{T^2} + \ln(\Phi) \tag{8}$$

where the constants, a, b and c, are utilized in the following expressions to obtain the desired thermodynamic quantities:

$$\Delta H = -R\left(b + \frac{2c}{T}\right) \tag{9}$$

$$\Delta S = R\left(a - \frac{c}{T^2}\right) \tag{10}$$

$$\Delta C_p = \frac{2Rc}{T^2} \tag{11}$$

Note that the non-linearity in this case originates from a non-zero value of ΔC_p. It is also important to point out that Eqs. (7)–(11) assume isocratic mobile phase elution conditions.

3. Experimental

3.1. Reagents and materials

HPLC grade perchloric acid (70% (w/w) in water) and HPLC grade acetonitrile were purchased from commercial sources (Aldrich and EMD Chemicals Inc., respectively). HPLC grade water was provided via a Picotech® Hydro® Ultrapure Water System. The active pharmaceutical ingredients, Compounds A, B, C and D, were manufactured in-house by the Chemical Process Development & Commercialization (CPDC) department and all were established to be >99.5% pure by the Analytical Development & Commercialization (ADC) department, Merck & Co., Inc.

3.2. Apparatus

All HPLC "reaction chromatograms" were acquired on an Agilent 1100 series HPLC system equipped with a diode array UV–vis detector monitoring the 250 nm wavelength, using Atlas 8.2 software (Thermo). An external Selerity Technologies Inc.® Series 9000™ oven (equipped with a mobile phase pre-heater) was used to maintain the column at the desired temperature, to perform all isothermal kinetic and thermodynamic experiments. For all runs, the column effluent was cooled to 25 °C prior to entry into the detector flow-cell. An Agilent mass-selective (MS) detector operated in electrospray ionization, ESI, mode (with formic acid in the aqueous mobile phase in place of the perchloric acid in the method described below) was used to identify the degradation products of the on-column reaction of Compound A.

3.3. Chromatographic method

Separations were performed using a ZirChrom® Diamondbond™-C18 column (150 mm × 4.6 mm, 3 μm particles), unless otherwise stated, utilizing a mobile phase consisting of two solvents: Solvent A—aqueous perchloric acid (0.1%, v/v) and Solvent B—HPLC grade acetonitrile. The gradient program started at 80A:20B (v/v), and achieved 20A:80B (v/v), over 30 min. A 5 min re-equilibration period (using 80A:20B (v/v)) was performed between sample injections. The flow rate was maintained at 1.0 mL/min for all runs.

3.4. On-column degradation of Compound A

Reaction chromatograms were collected using the above method at column temperatures in the range 40–200 °C, by injecting a standard solution of Compound A onto the column. To prepare the standard solution, Compound A was dissolved in acetonitrile–water (50:50, v/v) at a concentration of 1.0 mg/mL. An injection volume of 10 μL was used to introduce the sample. The sample tray was maintained at 10 °C to minimize the solvolysis of the sample between injections. With each incremental 10 °C change in the oven temperature, the column was allowed to equilibrate for a minimum of 30 min prior to injection of the standard solution. For each reaction chromatogram (obtained at each different T), the peak area of the Compound A "reactant" was integrated and recorded. The retention time of the API was also recorded. To obtain an estimate for the phase ratio at each column temperature (note: Φ should not be expected to be constant at different temperatures [13]), the flow rate, void elution time (t_0) and column dimensions were utilized in a standard manner to determine the hold-up volume [14]. The void elution time was determined using the change in refractive index caused by sample injection, which produced a baseline disturbance in each reaction chromatogram. Care was taken to ensure that t_0 was measured the same way in all chromatograms.

4. Results and discussion

4.1. Compound A: kinetics of on-column degradation and thermodynamics of retention

Fig. 2 shows a plot of the relative peak area counts of Compound A obtained as a function of the column temperature, using the HT-HPLC reactor. One can see that as the oven temperature is increased, the relative peak area decreases in a generally sigmoidal fashion (keep in mind that the reaction/retention time, t_R, also changes with T). From the overlay of reaction chromatograms in Fig. 3, it is possible to observe that this decrease in relative peak area comes as a result of the formation of multiple degradation products. The simultaneous decrease in t_R at elevated T is an expected trend for predominantly enthalpically

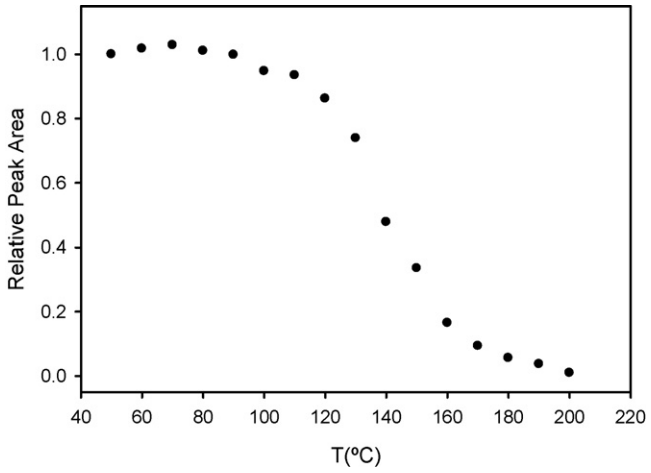

Fig. 2. Profile of the relative peak areas of Compound A plotted as a function of the column temperature, over the entire range of temperatures investigated using the HT-HPLC reactor (ZirChrom® Diamondbond™-C18 column). The loss in peak area at higher temperatures is indicative of Compound A degradation.

Table 1
HT-HPLC reactor data for the on-column degradation of Compound A

t_R (s)	t_0 (s)	T (K)	A_0	A	$1/T$ (K^{-1})	$\ln[(1/t_R)(1/A - 1/A_0)]$
1123	104	313	10,825	10,825	0.00319	N/A
1073	102	323	10,825	10,717	0.00310	−20.87
1025	101	333	10,825	10,677	0.00300	−20.50
977	99	343	10,825	10,355	0.00291	−19.27
926	98	353	10,825	10,261	0.00283	−19.02
873	94	363	10,825	9,484	0.00275	−18.02
819	93	373	10,825	8,188	0.00268	−17.13
765	92	383	10,825	6,820	0.00261	−16.46
709	91	393	10,825	4,726	0.00254	−15.60
655	89	403	10,825	3,456	0.00248	−15.02
599	88	413	10,825	1,981	0.00242	−14.19
545	88	423	10,825	1,545	0.00236	−13.80
487	86	433	10,825	1,083	0.00231	−13.28
434	87	443	10,825	494	0.00226	−12.32
385	85	453	10,825	495	0.00221	−12.21
340	83	463	10,825	353	0.00216	−11.73
298	82	473	10,825	279	0.00211	−11.35

The data were used to construct the plot in Fig. 4. Note that t_0 represents both the elution time of components that are not retained on the column and the reaction time of Compound A in the mobile phase (only). The other variables are defined as per the text. N/A = not applicable.

retained compounds (note that t_0 also diminishes at higher T due to mobile phase thermal expansion increasing the linear velocity; the simultaneous changes in t_0 and t_R as a function of T are accounted for in Eq. (7)).

Table 1 summarizes the chromatographic reactor data of interest for use in the kinetic treatments described earlier. As it was found that the data plotted using Eq. (5) was able to be fit by linear regression analysis much better than when plotted using Eq. (1) ($R^2 = 0.995$ versus 0.983; while the latter plot is not shown, the trend is visibly non-linear), the kinetics appear to be second-order (see Fig. 4). Such kinetic behavior might support the formation of an API dimer in the degradation mechanism of Compound A (discussed more below). Alternatively, the observation of second-order kinetics (first-order in reactant/API is normally expected for most degradation/thermal decomposition mechanisms) might indicate an experimental artifact (discussed more in the next section). Note that as the linear regression fit has a single slope, there does not appear to be any change in the degradation mechanism over the entire temperature range investigated. From the plot in Fig. 4, an apparent activation energy of 85.7 ± 1.6 kJ/mol and an apparent frequency factor of $(3.9 \pm 0.4) \times 10^4$ s^{-1} were extracted.

MS detection was used to try to identify the product peaks observed in the reaction chromatograms of Compound A, at elevated column temperatures (refer to Fig. 3). However, as the mobile phase composition of the chromatographic method had to be altered for use with MS (to utilize a volatile acid, formic acid, in the mobile phase instead of the perchloric acid; see Section 3), an exact correlation between the product peaks observed using UV detection and those seen in the total ion chromatograms (TICs; not shown) could not be obtained. Due to the different effective pHs provided by the different acids at elevated temperatures, somewhat different analyte retention times (and response factors) can be expected. Nonetheless, Fig. 5 shows proposed

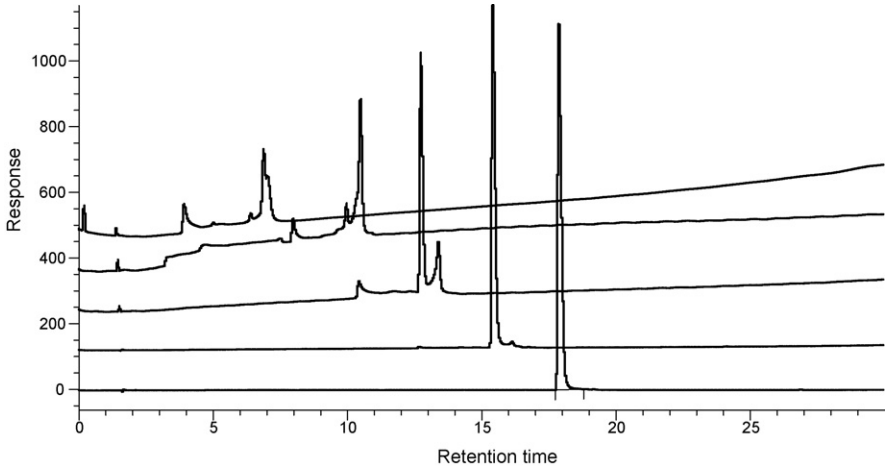

Fig. 3. Overlay of reaction chromatograms for the on-column degradation of Compound A (largest peak in bottom chromatogram). The column temperature increases from bottom to top: 50, 80, 110, 140 and 180 °C. The retention time has units of minutes; the UV detector response has arbitrary units (a.u.) of absorbance.

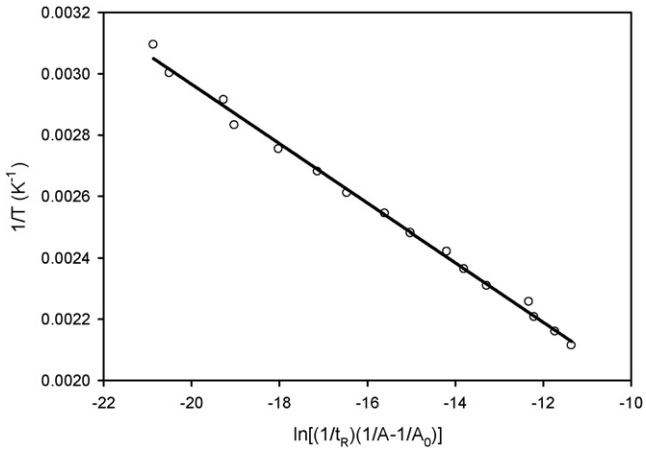

Fig. 4. Plot of $1/T$ vs. $\ln\left(\frac{1}{t_R}\left(\frac{1}{A}-\frac{1}{A_0}\right)\right)$ for the on-column degradation of Compound A, using data from Table 1. The linear regression fit ($R^2 = 0.995$) has a slope of -9.7×10^{-5} K^{-1} and a y-intercept of 1.0×10^{-3} K^{-1}.

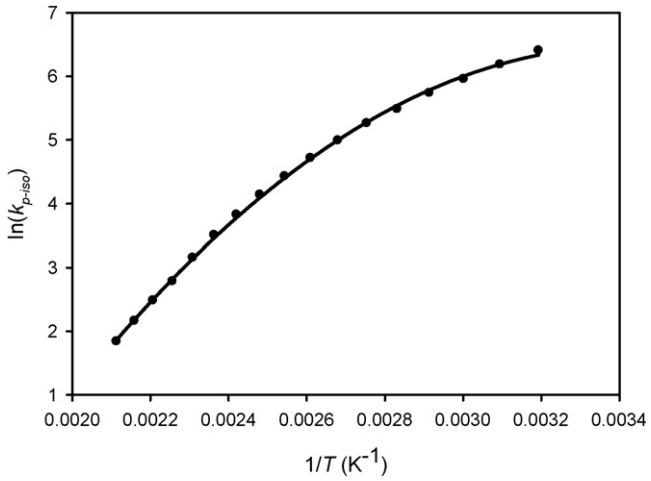

Fig. 6. Van't Hoff plot of the retention behavior of Compound A on the ZirChrom® Diamondbond™-C18 column. The data points were modeled using a regression fit to Eq. (8) in the text; refer to Table 2 for the relevant thermodynamic parameters extracted from the fit.

structures for two of the product peaks that were found to ionize under the experimental conditions used in this work. Interestingly, a "Compound A dimer" was also observed. Note that MS was also able to verify API peak purity/homogeneity, to ensure that there were no co-eluting degradation products.

For routine application of the HT-HPLC reactor approach, use of the perchloric acid mobile phase additive proved to be useful in providing a clean, stable baseline for the majority of temperatures utilized in this work. However, in order to facilitate the regular identification of degradation products (which is not necessary to obtain the kinetic trends presented and discussed here), the use of an MS-compatible acid modifier would be desirable for future studies.

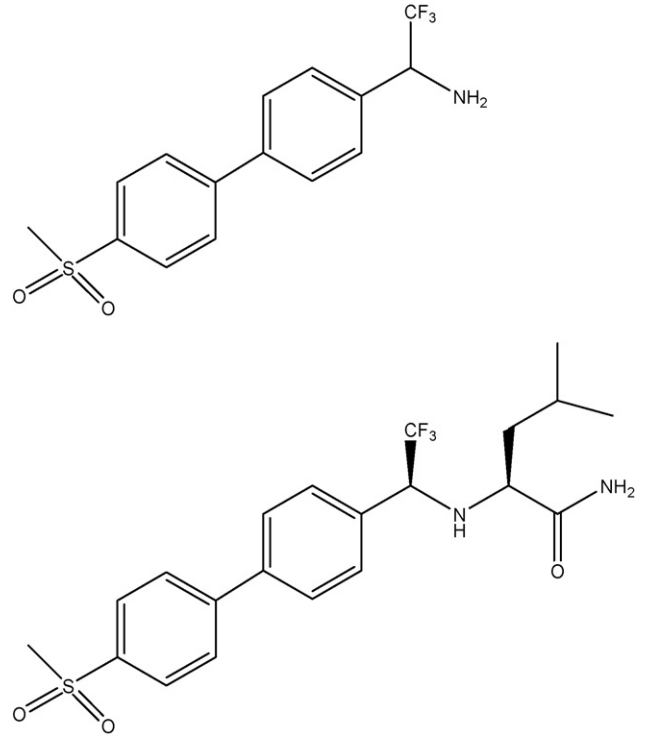

Fig. 5. Molecular structures of two of the Compound A degradation products observed using MS detection. Not shown is the Compound A dimer.

The van't Hoff plot in Fig. 6 shows distinct curvature, with an extrapolated maximum at ~20 °C (obtained by taking the derivative of the regression fit line and setting the slope equal to 0, then solving for T^{-1}). At that temperature, the retention mechanism for Compound A goes from being predominantly enthalpically driven to entropically driven. This transition temperature is quite close to that which is attributed to C-18 stationary phase orientation changes on silica particles [15], which occurs in the vicinity of the melting temperature of neat octadecane (23 °C) [13]. Thus, the observed transition temperature is consistent with a similar C-18 orientation change occurring on the zirconia phase. The finding that the C-18 chain transition temperature is largely independent of the chemical nature of the underlying particle (i.e., zirconia versus silica) might be of interest.

Treatment of the retention data with the aid of Eqs. (8)–(11) yielded the thermodynamic quantities that are summarized in Table 2. Note, however, that since the reaction chromatograms were collected under gradient conditions, the retention factors obtained experimentally had to be converted to equivalent "isocratic k_p" values, prior to constructing the plot in Fig. 6. To do that, one must determine the effect of mobile phase composition on the retention time of Compound A, i.e., the value of the parameter "β" in the equation below (assumed to be temperature-independent):

$$\beta = \frac{\mathrm{d}\ln(k_p)}{\mathrm{d}[\mathrm{MeCN}]} \tag{12}$$

That is because β is a key factor in the following equation:

$$\left(\frac{\mathrm{d}\ln(k_p)}{\mathrm{d}[\mathrm{MeCN}]}\right)\left(\frac{\mathrm{d}[\mathrm{MeCN}]}{\mathrm{d}t}\right) = \frac{\mathrm{d}\ln(k_p)}{\mathrm{d}t} \tag{13}$$

from which, using the fact that the gradient corresponds to a 2% (v/v) change in [MeCN] per minute (see Section 3) and

Table 2
Thermodynamic retention parameters for Compound A on the ZirChrom® Diamondbond™-C18 column, obtained using a regression fit of Eq. (8) to the curved data trend shown in Fig. 6

T (°C)	ΔH (kJ/mol)	ΔS (J K^{-1} mol^{-1})	ΔC_p (J K^{-1} mol^{-1})
40	−10.0 (±0.93)	27.4 (±14)	−460 (±17)
50	−14.5 (±0.76)	12.9 (±14)	−432 (±16)
60	−18.7 (±0.61)	−0.16 (±13)	−407 (±15)
70	−22.6 (±0.46)	−12.3 (±13)	−383 (±14)
80	−26.4 (±0.32)	−23.3 (±12)	−362 (±13)
90	−29.9 (±0.19)	−34.0 (±12)	−342 (±13)
100	−33.2 (±0.071)	−43.3 (±12)	−324 (±12)
110	−36.4 (±0.046)	−52.0 (±11)	−307 (±11)
120	−39.4 (±0.16)	−60.0 (±11)	−292 (±11)
130	−42.2 (±0.26)	−67.4 (±11)	−278 (±10)
140	−44.9 (±0.36)	−74.3 (±11)	−264 (±9.8)
150	−47.5 (±0.46)	−80.6 (±10)	−252 (±9.3)
160	−50.0 (±0.55)	−86.6 (±10)	−241 (±8.9)
170	−52.0 (±0.63)	−91.9 (±10)	−230 (±8.5)
180	−54.6 (±0.72)	−97.4 (±9.8)	−220 (±8.1)
190	−56.7 (±0.80)	−102 (±9.6)	−210 (±7.8)
200	−58.8 (±0.87)	−107 (±9.4)	−202 (±7.4)

Error estimates are provided in parentheses.

integrating, one can obtain the relation:

$$\ln(k_{p\text{-iso}}) = \ln(k_{p\text{-grad}}) - \frac{\beta}{30}(t_R - t_0) \quad (14)$$

where the subscripts "iso" and "grad" serve to denote isocratic and gradient elution conditions, respectively, and where the units of time have been selected to be seconds. Essentially, Eq. (14) uses the factor β and knowledge of the method gradient conditions to convert the retention factor of Compound A from gradient to isocratic conditions. Doing so allows for the direct application of Eqs. (8)–(11), described in Section 1.

In this work, it was determined that β is 0.121 at 50 °C and 0.127 at 150 °C (see Fig. 7). In each case, $R^2 > 0.995$ for the four data points collected at each temperature, using the different (isocratic) Solvent A/Solvent B compositions plotted in the figure. The two values are considered equivalent, within experimental error. For that reason, the average value of 0.124 was used in Eq. (14) to obtain the isocratic retention factors plotted in Fig. 6.

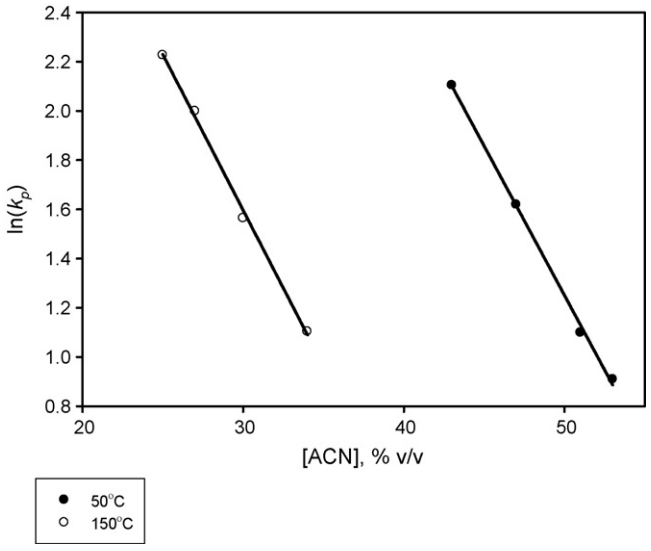

Fig. 7. Plots used to obtain the parameter, β (see Eq. (12) in the text), for converting the experimentally determined retention factors obtained for Compound A from gradient to isocratic conditions.

As an aside, it is likely not feasible to perform chromatographic experiments over the wide temperature range investigated in this work (40–200 °C) in an isocratic manner (at fixed mobile phase composition) due to the substantial method run time that would be required to do so, particularly at the lower temperatures; temperature typically has a significant impact on the retention times of compounds. In order to ensure API/degradation product elution inside of a 30 min window at all column temperatures (to reduce cycle time and to minimize peak broadening), yet obtain reasonable retention/separation, the use of a gradient method is desirable. Note, however, that one must assume that the analyte response factors change negligibly with changes in mobile phase composition over the entire elution window, using the present kinetic treatment (Eqs. (5) and (6)).

4.2. Toward the general application of the HT-HPLC reactor approach: kinetic investigations using other APIs

In order to evaluate the general gradient method and HT-HPLC reactor approach described in Section 3 for broader application to the screening of API stability/lability, three additional compounds, of varying size, geometry and containing different functional groups, were investigated. These molecules are depicted schematically in Fig. 8.

From Fig. 9, one can see that of the four APIs discussed in this work only two behave in the expected manner: the relative peak areas of Compounds A and D (Emend™) both exhibit the general sigmoidal dependence on the column temperature that can be predicted theoretically. Contrastingly, Compound B shows an unusual characteristic in that the peaks areas measured between ~60 and ~90 °C are greater than those measured at the initial column temperature. Even more extreme is the behavior of Compound C: the API peak seems to "disappear" at temperatures ranging from ~90 to ~120 °C, only to reappear and subsequently plateau at temperatures >155 °C. The strange on-column behavior of these two compounds relates non-physical kinetic interpretations of the data, barring any additional insights into the experimental system. Fortunately, a possible explanation for this behavior might reside in considering the Lewis acid/Lewis base properties of Compounds B and C.

From the literature, it is known that Lewis bases are problematic for use with zirconia-based columns in that they can adsorb irreversibly to these stationary phases [4–6]. From Fig. 8, one can see that Compound C is a potassium salt that readily dissociates under mobile phase/diluent conditions to form the neutral free base, which can then interact with the stationary phase as a Lewis base (predominantly, over the temperature range mentioned earlier). On the other hand, it is hypothesized here that Compound B exhibits complementary Lewis *acid*-like characteristics, mainly over a lower temperature range than over which Compound C exhibits the strong Lewis base-like prop-

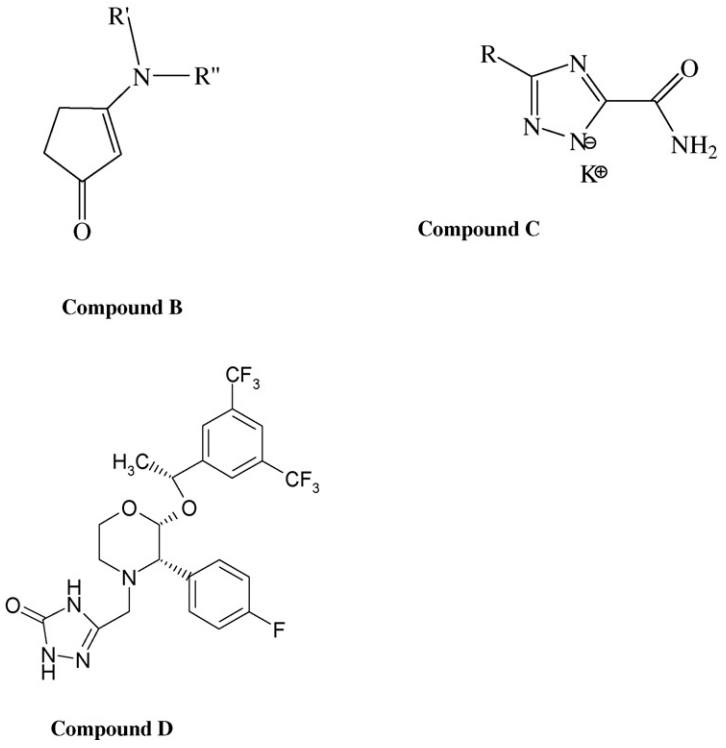

Fig. 8. Molecular structures of the other APIs investigated in this work, using the chromatographic reactor approach for studying degradation kinetics. Ambiguous "R groups" were added to two of the chemical structures to protect the identities of compounds currently under active development.

erties (discussed more below). While both behaviors appear to be reversible at the higher temperatures studied, fundamentally, such characteristics (artifacts) make it nearly impossible to investigate the degradation kinetics of these APIs, using the present set-up.

Both Compounds A and C can be expected to be neutral under the mobile phase conditions described in Section 3. However, only the latter molecule possesses a strongly basic moiety that can affect the peak area trends in the manner observable in Fig. 9. In comparison, while Compounds B and D are structurally analogous in many respects (and they can both be expected to be protonated under the mobile phase conditions due to the presence of a tertiary amine), the latter molecule contains a triazolone group while Compound B has a terminal cyclopentenone moiety. The cyclopentenone group, unlike triazolone, is thought to serve as an electron acceptor (i.e., a Lewis acid) when it interacts with the zirconia phase, producing the effect seen in Fig. 9 by counteracting/overcoming any (weaker) Lewis base interactions of the API molecule, primarily observed at lower *T*. This idea stems from the fact that Compound B is known to hydrolyze via the cleavage of the cyclopentenone group, following nucleophilic attack by an electron donor/Lewis base. To summarize, the different Lewis acid/base properties of the various APIs used in this study appear to support the unusual chromatographic behavior depicted in the figure.

The bizarre on-column behavior observed for Compounds B and C led to additional studies using a Hamilton^{TM} PRP-1$^{®}$ column (150 mm × 4.6 mm, 5 μm particles), in place of the zirconia-based column described in Section 3 (keeping all other method parameters essentially unchanged). As can be seen from Fig. 10, the polymeric column produced more expected peak area versus temperature trends for both of these APIs. However, while eliminating the artifacts noted in Fig. 9 (which can hence be inferred to be attributable to the zirconia stationary phase, and not complications stemming from changes in the API response factors due to elution time variation as a function of *T*, for example, or, alternatively, from degradation products co-eluting with the API peak), the PRP-1 column is limited by

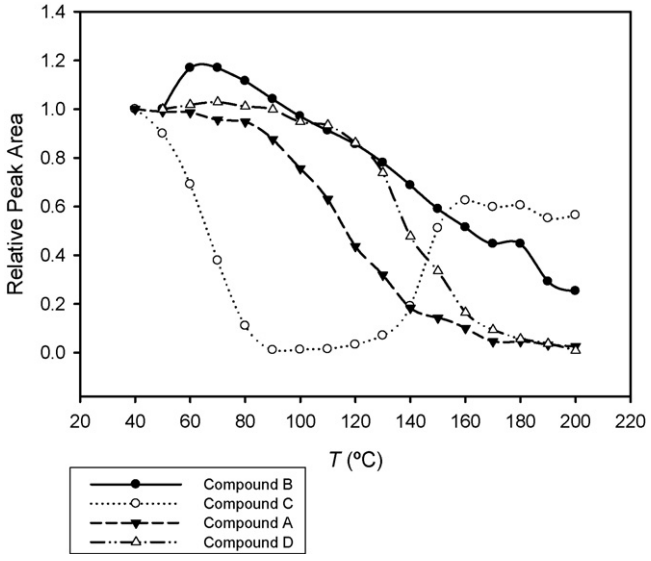

Fig. 9. Overlay of the relative peak area vs. column temperature profiles obtained for Compounds A–D over the entire range of temperatures investigated (ZirChrom® Diamondbond^{TM}-C18 column); lines added to guide the reader.

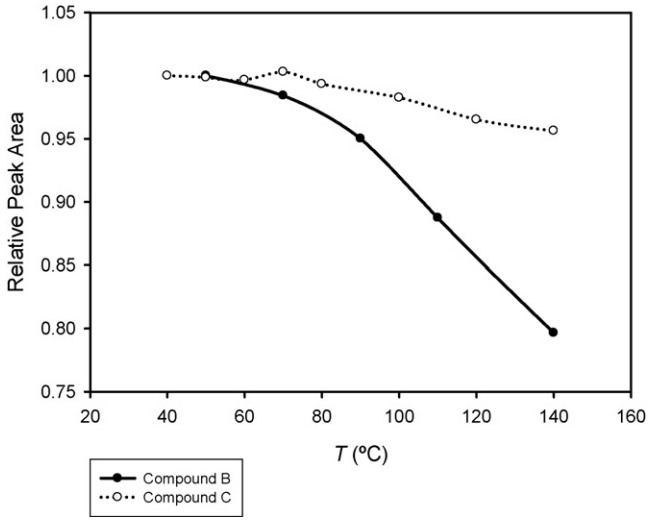

Fig. 10. Overlay of the relative peak area vs. column temperature profiles obtained for Compounds B and C over the temperature range 40–140 °C, using the Hamilton™ PRP-1® column (lines added to guide the reader).

an upper operating temperature of only 80 °C, as specified by the manufacturer (the authors intentionally exceeded that temperature in their study, by almost twofold, but the short excursions did not appear to detrimentally affect the column performance). Thus, use of this column can reduce the range of API chemical stabilities/reactivities that can be routinely probed and/or the extent of degradation that can be observed (in < 60 min run time), using the chromatographic reactor technique described herein. Graphitic columns [16,17], which can supposedly withstand temperatures above 200 °C, were not evaluated in this work; they are left for future evaluation.

5. Conclusions

The liquid chromatographic reactor approach can be effective for studying elementary reaction kinetics such as the thermal decomposition of various APIs (via hydrolysis or solvolysis pathways). That is the case because the approach greatly reduces the number of chromatograms that must be collected and analyzed in order to obtain a complete kinetic characterization (i.e., the activation energy and frequency factor, together) of a given reaction, when used in conjunction with the mathematical treatments provided by the authors in this work and in previous papers. However, attempting to use the HT-HPLC approach to access the kinetics of more thermodynamically stable compounds comes with certain limitations of which the analyst should be aware. For example, zirconia-based stationary phases can produce unexpected kinetic trends for molecules containing either Lewis base or Lewis acid moieties. The use of polymer-based stationary phases can reduce the number and likelihood of such artifacts, but they might substantially limit the upper operating temperature of the kinetic experiments.

Acknowledgements

The authors would like to thank the MMD Science & Technology Development department for funding A.B. through the Merck summer internship program.

References

[1] P.J. Skrdla, A. Abrahim, Y. Wu, J. Pharm. Biomed. Anal. 41 (2006) 883–890.
[2] C.Y. Jeng, S.H. Langer, J. Chromatogr. 589 (1992) 1–30.
[3] O. Trapp, Anal. Chem. 78 (2006) 189–198.
[4] R. Kučera, V. Žižkovsky, J. Sochor, J. Klimeš, J. Dohnal, J. Sep. Sci. 28 (2005) 1307–1314.
[5] K. Soukupová, E. Krafková, J. Suchánková, E. Tesařová, J. Chromatogr. A 1087 (2005) 104–111.
[6] F. Cacciola, P. Jandera, L. Mondello, J. Sep. Sci. 30 (2007) 462–474.
[7] P.J. Skrdla, Int. J. Chem. Kinet. 36 (2004) 386–393.
[8] P.J. Skrdla, V. Antonucci, C. Lindemann, J. Chromatogr. Sci. 39 (2001) 431–440.
[9] P.J. Skrdla, R.T. Robertson, J. Mol. Catal. A 194 (2003) 255–265.
[10] P.J. Skrdla, C. Lindemann, Appl. Catal. A 246 (2003) 227–235.
[11] L. Wright, P.J. Skrdla, V. Antonucci, N. Variankaval, Chromatographia 58 (2003) 405–409.
[12] D. Haidacher, A. Vailaya, C. Horváth, Proc. Natl. Acad. Sci. 93 (1996) 2290–2295.
[13] T.L. Chester, J.W. Coym, J. Chromatogr. A 1003 (2003) 101–111.
[14] T. Ahmad, G. Guiochon, J. Chromatogr. A 1129 (2006) 174–188.
[15] L.A. Cole, J.G. Dorsey, K.A. Dill, Anal. Chem. 64 (1992) 1324–1327.
[16] J. Li, P.W. Carr, Anal. Chem. 69 (1997) 3884–3888.
[17] S. Yamaki, T. Isobe, T. Okuyama, T. Shinoda, J. Chromatogr. A 728 (1996) 189–194.